

SPACECRAFT MANEUVERING VIA ATMOSPHERIC DIFFERENTIAL DRAG USING AN ADAPTIVE LYAPUNOV CONTROLLER

D. Pérez,^{*} and R. Bevilacqua[†]

An atmospheric differential drag based adaptive Lyapunov controller, originally proposed by the authors in previous work for spacecraft rendezvous, is here generalized allowing for the tracking of reference trajectories or dynamics. Differential drag is based on the ability to vary a satellite's cross wind surface area, and it represents a propellant-free alternative to thrusters to control relative motion of low Earth orbiting spacecraft. The interest in autonomous propellant-less maneuvering comes from the desire of reducing costs of performing formation maneuvering. Formation maneuvering opens up a wide variety of new applications for spacecraft, such as on-orbit maintenance missions and refueling. The control technique is successfully tested using Systems Tool Kit simulations for re-phase, fly-around, and rendezvous maneuvers, proving the feasibility of the proposed approach for a real flight.

INTRODUCTION

An adaptive Lyapunov control technique, originally proposed in previous work^{1,2} for a rendezvous maneuver using differential drag, is further developed and generalized allowing for the tracking of reference trajectories or dynamics. The control algorithm is tested using Systems Tool Kit (STK) simulations for re-phase (regulating), fly-around (trajectory tracking) and rendezvous maneuvers (tracking a reference model). The interest in autonomous propellant-less maneuvering comes from the desire for reducing costs of performing formation maneuvering. Formation maneuvering opens up a wide array of new applications for spacecraft, such as on orbit maintenance missions and refueling. Successful autonomous propellant-less maneuvering of low Earth orbit (LEO) spacecraft on the orbital plane can be achieved using differential drag.

The idea of using differential drag for controlling the relative motion of spacecraft was first introduced by C.L. Leonard³. The ORBCOMM constellation of LEO satellites was the first one to use differential drag for formation keeping⁴; while, the JC2Sat project developed by the Canadian and Japanese Space Agencies^{5,6} was an envisioned application of these ideas.

Control of spacecraft formation maneuvers is an increasingly important topic given the potential for its application for autonomous guidance of satellite swarms, refueling, autonomous as-

^{*} Ph. D. Candidate, Mechanical, Aerospace and Nuclear Engineering Department, 110 8th Street, Troy, NY 12180, USA. perezd3@rpi.edu

[†] Assistant Professor, Mechanical, Aerospace and Nuclear Engineering Department, 110 8th Street, Troy, NY 12180, USA. bevilr@rpi.edu. www.riccardobevilacqua.com

sembly of structures in space and on-orbit maintenance missions. The latter has been specifically targeted by NASA through its Satellite Servicing Capabilities Office ⁷.

The variation in the drag can be induced, for example, by deploying or retracting a surface (see Figure 1), hence effectively modifying the spacecraft's ballistic coefficient. The reference frame commonly employed for spacecraft relative motion representation is the Local Vertical Local Horizontal (LVLH) reference frame, where x points from Earth to the reference spacecraft (virtual or real), y points along the track (direction of motion), and z completes the right-handed frame (see Figure 1). The differential acceleration generated by deploying/retracting a surface is approximated to the y component only¹, limiting controllability to the x - y plane.

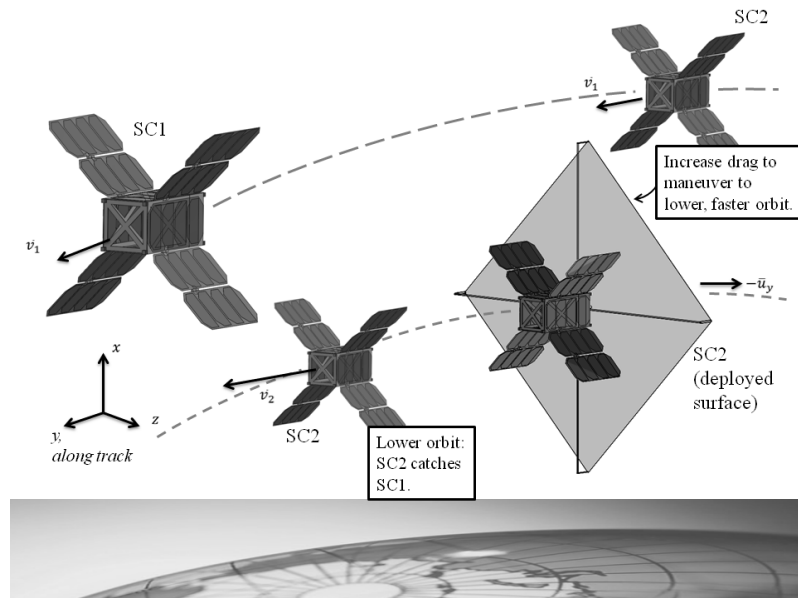


Figure 1. Drag surface deployment concept to generate differential drag

The magnitude of the differential drag acceleration fluctuates during the maneuver as the spacecraft encounters regions of the thermosphere (85 km above the Earth) with different atmospheric densities. In the thermosphere, atmospheric density can change significantly due to solar activity. These variations are difficult to model and measure accurately on board; hence, robust control strategies must be designed to increase the reliability of spacecraft maneuvering using differential drag.

The problem of designing a control system for in plane maneuvering using differential drag becomes the problem of designing a real-time control law to command the deployment or retraction of the surfaces attached to the target and chaser spacecraft, with the intent of forcing the spacecraft to follow a desired trajectory, a linear reference model, or simply regulate to a final desired state. A stable linear reference model is introduced; this model tracks the desired rendezvous trajectory. The Lyapunov controller can then be used to either directly track the desired trajectory or track the dynamics of the linear reference model. In previous work, ⁸ a Lyapunov controller was developed for addressing this problem. In essence, a Lyapunov function of the tracking error is selected, and the control signal is chosen so that the tracking error converges to zero (i.e. the first order time derivative of the Lyapunov function is negative). Thus, the nonlinear dynamics of the system are forced to follow a desired trajectory. This significantly simplifies the control problem, since the desired trajectory can be designed using controlled linear dynamics approximating the reality of spacecraft relative motion. The possibility of tracking different tra-

jectories or a reference dynamic allows this controller to be used for many different relative maneuvers using differential drag, provided that they are constrained to the orbital plane.

In later work the Lyapunov controller was improved by introducing an adaptation to reduce control effort and maneuver duration for a rendezvous maneuver^{1,2}. An analytical expression for the differential drag acceleration critical value that ensures stability in the sense of Lyapunov for the system was found, and partial derivatives of this critical value in terms of \underline{Q} (Lyapunov equation matrix), and \underline{A}_d (reference linear dynamics matrix) were also developed in^{1,2}, only for the regulation case. Furthermore, an adaptation that chooses in real time an appropriate positive definite matrix \underline{P} in a quadratic Lyapunov function, by modifying the \underline{Q} and \underline{A}_d matrices based on the partial derivatives was developed. Nonetheless, the adaptation could only be utilized when the controller was used for regulation, since the partial derivatives were developed for that case only and consequently, the spacecraft could only go from an initial state to a final state without following any desired path; thus, restricting the application of the controller.

In this paper, the adaptive Lyapunov controller presented in^{1,2} is generalized to force the spacecraft to follow trajectories and linear reference dynamics, provided that they are physically realizable, i.e. they evolve in time scales comparable to those typical of differential drag.

As a simplification, the control law is based on the assumption that the control is either positive maximum, negative maximum, or zero, as previously done in^{1,2,8} and⁹, neglecting the time required by the surfaces to be deployed or retracted. This simplification is valid since the time required to deploy or retract the surfaces (in the order of seconds, or minutes at the most) is negligible with respect to the maneuvers durations (in the order of days).

The foremost contributions of this work are:

- 1) Analytical expressions for the partial derivatives of the critical value of the differential drag acceleration in terms of \underline{Q} (Lyapunov equation matrix), and \underline{A}_d (reference linear dynamics matrix) for the general case in which the spacecraft are tracking a linear reference model, which can also be used for tracking a guidance trajectory or a desired final state (regulation).
- 2) Simulations that validate the adaptive Lyapunov controller for three different maneuvers; Fly-around, Re-Phase, and Rendezvous, via Systems Tool Kit (STK) numerical simulations.
- 3) Assessment of the performances of the designed adaptive Lyapunov control strategy for the three different maneuvers in terms of the duration of the rendezvous maneuver and the number of deployments/retractions (control effort), in comparison with the non-adaptive Lyapunov control strategy previously presented by the authors⁸.
- 4) Overall, this paper provides a valuable generalization of the work presented in⁸ which allows for propellant less autonomous relative maneuvers within the orbital plane.

The paper is organized as follows. Section II presents the concept of atmospheric differential drag. Section III presents the spacecraft relative motion linear and nonlinear dynamics employed in the following developments. Section IV is dedicated to the Lyapunov control law, as well as the general analytical derivatives of the differential drag critical value with respect to the independent variable matrices. Section V presents the results of the simulations of the three different maneuvers performed in STK, and Section VI draws the conclusions.

II. DIFFERENTIAL DRAG

The drag acceleration experienced by a spacecraft at LEO is a function of the atmospheric density, atmospheric winds, velocity of the spacecraft relative to the medium, and the geometry, attitude, drag coefficient and mass of the spacecraft. The interdependence of these parameters (e.g. the drag coefficient is affected by the temperature of the medium which also determines the density of the medium) and the lack of knowledge in some of their dynamics make the modeling of the drag force a challenging and still largely unsolved problem. This results in large uncertainties regarding the control forces available for maneuvers using drag forces. Consequently the control systems used for drag maneuvers must be able to cope with these uncertainties.

The aerodynamic acceleration experienced by a spacecraft is typically decomposed into the lift (lift forces are negligible at LEO) and drag forces, the latter usually expressed as:

$$a_d = \frac{1}{2} \rho BC v_s^2 \quad (1)$$

where ρ is the atmospheric density, and v_s is the velocity of the spacecraft relative to the atmospheric particles. The ballistic coefficient BC is given by:

$$BC = \frac{C_D A}{m} \quad (2)$$

where C_D is the drag coefficient of the spacecraft, A is the cross-wind surface area of the spacecraft, and m is the mass of the spacecraft.

Using Eq. (1), the magnitude of the relative acceleration caused by the differential aerodynamic drag for the spacecraft system (target and chaser) is given as:

$$a_{Drel} = \frac{1}{2} \rho \Delta BC v_s^2 \quad (3)$$

where ΔBC is the difference in ballistic coefficients between the target and chaser.

In the thermosphere, the solar activity creates large variations of temperature, which drive variations of the atmospheric density. These variations produce significant changes in the available magnitude of drag acceleration for a given ballistic coefficient.

III. LINEAR REFERENCE AND NONLINEAR MODELS

The effect of the J_2 perturbation and other nonlinearities is more significant in maneuvers with longer times of execution, such as those performed using differential drag. For this reason the use of a linear model that partially accounts for averaged effects of these nonlinearities is desired, like the one described in the following section. The model described in the following section is used for the derivation of the Lyapunov controller.

Linear Reference Model

A linearized model which represents the relative motion of spacecraft under the influence of the J_2 was developed by Schweighart and Sedwick¹⁰. Adding the control acceleration vector (\mathbf{u}) to the Schweighart and Sedwick equations, the following system of linear differential equations in the LVLH frame is obtained.

$$\dot{\mathbf{x}}_d = \underline{\mathbf{A}}\mathbf{x}_d + \underline{\mathbf{B}}\mathbf{u}, \quad \underline{\mathbf{A}} = \begin{bmatrix} \mathbf{0}_{2 \times 2} & \mathbf{I}_{2 \times 2} \\ b & 0 & 0 & a \\ 0 & 0 & -a & 0 \end{bmatrix}, \quad \underline{\mathbf{B}} = \begin{bmatrix} 0 \\ 0 \\ 0 \\ 1 \end{bmatrix}, \quad \mathbf{x}_d = \begin{bmatrix} x_d \\ y_d \\ \dot{x}_d \\ \dot{y}_d \end{bmatrix}, \quad (4)$$

$$a = 2nc, \quad b = (5c^2 - 2)n^2, \quad c = \sqrt{1 + \frac{3J_2 R}{8r_t^2} [1 + 3 \cos(2i_t)]}, \quad d = \sqrt{a^2 - b}$$

where n is the mean motion of the target, J_2 is the second zonal harmonic, R is the Earth mean radius, r_t is the target's orbit radius and i_t is the target's inclination. Noteworthy, the control action is only along the y direction, as depicted in Figure 1.

Since the dynamics of the Schweighart and Sedwick model are unstable, a Linear Quadratic Regulator (LQR) feedback controller is used to stabilize them and obtain the necessary linear model for Lyapunov developments. The resulting reference model is described by:

$$\dot{\mathbf{x}}_d = \underline{\mathbf{A}}_d \mathbf{x}_d + \underline{\mathbf{B}} \mathbf{u}_d, \quad \underline{\mathbf{A}}_d = \underline{\mathbf{A}} - \underline{\mathbf{B}} \underline{\mathbf{K}}, \quad \mathbf{u}_d = \underline{\mathbf{K}} \mathbf{x}_t \quad (5)$$

where $\underline{\mathbf{K}}$ is a constant matrix found by solving the LQR problem for the Schweighart and Sedwick model, thus ensuring $\underline{\mathbf{A}}_d$ to be Hurwitz, and \mathbf{x}_t is the desired guidance. For solving the LQR problem an identity matrix was used as the $\underline{\mathbf{Q}}_{LQR}$ matrix and R_{LQR} value was changed depending on the maneuver, since this value greatly determines the behavior of the stable linear reference model. Furthermore, the state vector \mathbf{x}_d is the desired reference dynamics, and control action is along the y direction only. This stable linear reference system can be regulated or forced to track a desired guidance trajectory.

Nonlinear Model

The dynamics of spacecraft relative motion are nonlinear due to effects, such as the J_2 perturbation and the nonlinear variations on the atmospheric density at LEO. The adaptive Lyapunov-based control intends to cope with these unmodeled effects by minimizing the differential drag critical value (minimum differential drag to have Lyapunov stable behavior) at all times, thus increasing the control margin. The nonlinear dynamics, including the J_2 perturbation, are defined as:

$$\dot{\mathbf{x}} = \mathbf{f}(\mathbf{x}) + \underline{\mathbf{B}}\mathbf{u}, \quad \mathbf{x} = [x \quad y \quad \dot{x} \quad \dot{y}]^T, \quad \mathbf{u} = \begin{cases} a_{Drel} \\ 0 \\ -a_{Drel} \end{cases} \quad (6)$$

where a_{Drel} acts along the y direction only, $\mathbf{f}(\mathbf{x})$ is an approximation of the full nonlinear relative motion dynamics, truncated to J_2 .

IV. ADAPTIVE LYAPUNOV CONTROL

Lyapunov Control Law

In previous work⁸ Lyapunov principles originally used in¹¹ were used to develop a criterion for the activation of the actuators of the surfaces which generate the differential drag. More specifically, the control signal is chosen such that the Lyapunov function (Eq. (7)) of the tracking error is positive, and the derivative of the Lyapunov function (Eq. (8)) is negative, thus ensuring that the tracking error converges to zero (as it was suggested in³). The Lyapunov controller can

be used to force the nonlinear model (i.e. the dynamics of the Target and Chaser Spacecraft) to directly track a desired constant final state, a desired guidance trajectory or the dynamics of a linear reference model as shown in earlier work ².

$$V = \mathbf{e}^T \underline{\mathbf{P}} \mathbf{e}, \quad \mathbf{e} = \mathbf{x} - \mathbf{x}_d, \quad \underline{\mathbf{P}} \succ 0 \quad (7)$$

$$\dot{V} = \mathbf{e}^T (\underline{\mathbf{A}}_d^T \underline{\mathbf{P}} + \underline{\mathbf{P}} \underline{\mathbf{A}}_d) \mathbf{e} + 2\mathbf{e}^T \underline{\mathbf{P}} (\mathbf{f}(\mathbf{x}) - \underline{\mathbf{A}}_d \mathbf{x} + \underline{\mathbf{B}} a_{Drel} \hat{u} + -\underline{\mathbf{B}} a_{Drel} \hat{u}_d) = -\mathbf{e}^T \underline{\mathbf{Q}} \mathbf{e} + 2(\beta \hat{u} - \delta) \quad (8)$$

where \hat{u} is the command sent to the surface actuators, matrices $\underline{\mathbf{A}}_d$ and $\underline{\mathbf{B}}$ represent the linear dynamics, matrix $\underline{\mathbf{Q}}$ is chosen such that a Lyapunov equation is satisfied ($\underline{\mathbf{A}}_d^T \underline{\mathbf{P}} + \underline{\mathbf{P}} \underline{\mathbf{A}}_d = -\underline{\mathbf{Q}}$), \mathbf{e} is the tracking error vector, \mathbf{x} and \mathbf{x}_d are defined as the actual spacecraft relative state vector and the reference state vector respectively, a_{Drel} is the magnitude of the differential drag acceleration, and $\mathbf{f}(\mathbf{x})$ accounts for all nonlinearities. The resulting control law presented in ⁸ can be expressed as:

$$\hat{u} = -\text{sign}(\mathbf{e}^T \underline{\mathbf{P}} \underline{\mathbf{B}}) \quad (9)$$

Critical value for the differential drag

An analytical expression for the critical value of the differential drag acceleration (Eq. (10)) that ensures stability in the sense of Lyapunov for the system was developed in prior work ¹. This was accomplished for the simplified case of regulation (no linear dynamics to track), by substituting $\delta = \mathbf{e}^T \underline{\mathbf{P}} \mathbf{f}(\mathbf{x})$ in Eq. (10). In the general case here addressed, the critical value expression is the following

$$a_{Dcrit} = \frac{\delta}{|\mathbf{e}^T \underline{\mathbf{P}} \underline{\mathbf{B}}|} = \frac{\mathbf{e}^T \underline{\mathbf{P}} (\underline{\mathbf{A}}_d \mathbf{x} - \mathbf{f}(\mathbf{x}) + \underline{\mathbf{B}} \mathbf{u}_d)}{|\mathbf{e}^T \underline{\mathbf{P}} \underline{\mathbf{B}}|} \quad (10)$$

General partial derivatives

In this work, the partial derivatives of the critical value in terms of matrices $\underline{\mathbf{A}}_d$ and $\underline{\mathbf{Q}}$ are generalized to the case in which the Lyapunov controller tracks a desired guidance or the dynamics of the reference model (δ includes all the terms shown in Eq. (10)). Thus, allowing the adaptive Lyapunov controller to track a desired guidance, the dynamics of the reference model, in addition to performing regulation.

For the development of the general matrix derivatives the following matrices were defined

$$\underline{\mathbf{U}}_1 = \sum_r \sum_s \underline{\mathbf{E}}_{rs} \otimes \underline{\mathbf{E}}_{rs}^T, \quad \underline{\mathbf{U}}_{n \times n} = \sum_r \sum_s \underline{\mathbf{E}}_{rs} \otimes \underline{\mathbf{E}}_{rs} \quad (11)$$

Where the matrix $\underline{\mathbf{E}}_{rs}$ is an elementary matrix with a one at position r,s and zeros elsewhere. Moreover, $\underline{\mathbf{I}}_{n \times m}$ is an n -by- m identity matrix. The matrix derivatives as defined in ¹² are described by:

$$\begin{aligned}
\frac{\partial \underline{\mathbf{Y}}}{\partial \underline{\mathbf{X}}} = \underline{\mathbf{Y}}, \underline{\mathbf{X}} &= \begin{bmatrix} (\underline{\mathbf{Y}}, X_{11}) & \dots & (\underline{\mathbf{Y}}, X_{1n}) \\ \vdots & \ddots & \vdots \\ (\underline{\mathbf{Y}}, X_{n1}) & \dots & (\underline{\mathbf{Y}}, X_{nn}) \end{bmatrix}, \quad \frac{\partial \underline{\mathbf{Y}}_v}{\partial \underline{\mathbf{X}}_v} = \text{vec}(\underline{\mathbf{Y}}), \text{vec}(\underline{\mathbf{X}}) = \begin{bmatrix} (\text{vec}(\underline{\mathbf{Y}}))^T, X_{11} \\ \vdots \\ (\text{vec}(\underline{\mathbf{Y}}))^T, X_{n1} \\ \vdots \\ (\text{vec}(\underline{\mathbf{Y}}))^T, X_{1n} \\ \vdots \\ (\text{vec}(\underline{\mathbf{Y}}))^T, X_{nn} \end{bmatrix}, \\
\frac{\partial \underline{\mathbf{Y}}_v}{\partial \underline{\mathbf{X}}} = \text{vec}(\underline{\mathbf{Y}}), \underline{\mathbf{X}} &= \begin{bmatrix} (\text{vec}(\underline{\mathbf{Y}}), X_{11}) & \dots & (\text{vec}(\underline{\mathbf{Y}}), X_{1n}) \\ \vdots & \ddots & \vdots \\ (\text{vec}(\underline{\mathbf{Y}}), X_{n1}) & \dots & (\text{vec}(\underline{\mathbf{Y}}), X_{nn}) \end{bmatrix}, \\
\frac{\partial [\underline{\mathbf{Y}}_v]^T}{\partial \underline{\mathbf{X}}} = [\text{vec}(\underline{\mathbf{Y}})]^T, \underline{\mathbf{X}} &= \begin{bmatrix} ([\text{vec}(\underline{\mathbf{Y}})]^T, X_{11}) & \dots & ([\text{vec}(\underline{\mathbf{Y}})]^T, X_{1n}) \\ \vdots & \ddots & \vdots \\ ([\text{vec}(\underline{\mathbf{Y}})]^T, X_{n1}) & \dots & ([\text{vec}(\underline{\mathbf{Y}})]^T, X_{nn}) \end{bmatrix}
\end{aligned} \tag{12}$$

Where the vectors $\underline{\mathbf{Y}}_v$ and $\underline{\mathbf{X}}_v$ are the vectorized (vec) versions of the matrices $\underline{\mathbf{Y}}$ and $\underline{\mathbf{X}}$. Also, the following matrix derivative transformations defined in ¹² are used

$$\begin{aligned}
\frac{\partial \underline{\mathbf{Y}}}{\partial \underline{\mathbf{X}}} &= \mathbf{T}_1 \left(\frac{\partial \underline{\mathbf{Y}}_v}{\partial \underline{\mathbf{X}}_v} \right), \quad \frac{\partial \underline{\mathbf{Y}}}{\partial \underline{\mathbf{X}}} = \mathbf{T}_2 \left(\frac{\partial \underline{\mathbf{Y}}_v}{\partial \underline{\mathbf{X}}} \right), \quad \frac{\partial \underline{\mathbf{Y}}}{\partial \underline{\mathbf{X}}} = \mathbf{T}_3 \left(\frac{\partial [\underline{\mathbf{Y}}_v]^T}{\partial \underline{\mathbf{X}}} \right), \\
\frac{\partial \underline{\mathbf{Y}}_v}{\partial \underline{\mathbf{X}}} &= \mathbf{T}_1^{-1} \left(\frac{\partial \underline{\mathbf{Y}}}{\partial \underline{\mathbf{X}}} \right), \quad \frac{\partial \underline{\mathbf{Y}}_v}{\partial \underline{\mathbf{X}}} = \mathbf{T}_2^{-1} \left(\frac{\partial \underline{\mathbf{Y}}}{\partial \underline{\mathbf{X}}} \right), \quad \frac{\partial [\underline{\mathbf{Y}}_v]^T}{\partial \underline{\mathbf{X}}} = \mathbf{T}_3^{-1} \left(\frac{\partial \underline{\mathbf{Y}}}{\partial \underline{\mathbf{X}}} \right)
\end{aligned} \tag{13}$$

Starting from Eq. (10), the general critical value is expressed as:

$$\begin{aligned}
a_{\text{Dcrit}} &= \eta(\underline{\mathbf{P}}) \psi(\underline{\mathbf{A}}_d), \\
\eta(\underline{\mathbf{P}}) &= \frac{\mathbf{e}^T \underline{\mathbf{P}}}{|\mathbf{e}^T \underline{\mathbf{P}} \mathbf{B}|}, \quad \psi(\underline{\mathbf{A}}_d) = \underline{\mathbf{A}}_d \mathbf{x} - \mathbf{f}(\mathbf{x}) + \mathbf{B} \mathbf{u}_d
\end{aligned} \tag{14}$$

where matrix $\underline{\mathbf{P}}$ is a function of matrices $\underline{\mathbf{A}}_d$ and $\underline{\mathbf{Q}}$ via the following Lyapunov equation

$$-\underline{\mathbf{Q}} = \underline{\mathbf{A}}_d^T \underline{\mathbf{P}} + \underline{\mathbf{P}} \underline{\mathbf{A}}_d \tag{15}$$

which as shown in ¹² can be rewritten as:

$$\begin{aligned}
\underline{\mathbf{P}}_v &= -\underline{\mathbf{A}}_v^{-1} \underline{\mathbf{Q}}_v, \\
\underline{\mathbf{A}}_v &= \mathbf{I}_{4 \times 4} \otimes \underline{\mathbf{A}}_d + \underline{\mathbf{A}}_d \otimes \mathbf{I}_{4 \times 4}, \quad \underline{\mathbf{P}}_v = \text{vec}(\underline{\mathbf{P}}), \quad \underline{\mathbf{Q}}_v = \text{vec}(\underline{\mathbf{Q}})
\end{aligned} \tag{16}$$

where \otimes represent the Kronecker product defined in ¹² for the same n-by-n $\underline{\mathbf{Y}}$ and $\underline{\mathbf{X}}$ matrices as:

$$\underline{\mathbf{X}} \otimes \underline{\mathbf{Y}} = \begin{bmatrix} (X_{11}\underline{\mathbf{Y}}) & \cdots & (X_{1n}\underline{\mathbf{Y}}) \\ \vdots & \ddots & \vdots \\ (X_{n1}\underline{\mathbf{Y}}) & \cdots & (X_{nm}\underline{\mathbf{Y}}) \end{bmatrix} \quad (17)$$

Also in ^{1,2}, the partial derivatives of $\underline{\mathbf{P}}$ in terms of $\underline{\mathbf{A}}_d$ and $\underline{\mathbf{Q}}$ were found; these derivatives are used in the following developments and can be expressed as:

$$\begin{aligned} \frac{\partial \underline{\mathbf{P}}}{\partial \underline{\mathbf{A}}_d} &= \mathbf{T}_2 \left(\left[\mathbf{T}_3^{-1} \left(\frac{\partial \underline{\mathbf{A}}_v}{\partial \underline{\mathbf{A}}_d} \right) \otimes \mathbf{I}_{16 \times 16} \right] \left[\mathbf{I}_{4 \times 4} \otimes \mathbf{T}_1^{-1} \left(\frac{\partial \underline{\mathbf{P}}_v}{\partial \underline{\mathbf{A}}_v} \right) \right] \right), \\ \frac{\partial \underline{\mathbf{A}}_v}{\partial \underline{\mathbf{A}}_d} &= (\mathbf{I}_{4 \times 4} \otimes \underline{\mathbf{U}}_1) (\underline{\mathbf{U}}_{4 \times 4} \otimes \mathbf{I}_{4 \times 4}) (\mathbf{I}_{4 \times 4} \otimes \underline{\mathbf{U}}_1) + \underline{\mathbf{U}}_{4 \times 4} \otimes \mathbf{I}_{4 \times 4}, \\ \frac{\partial \underline{\mathbf{P}}_v}{\partial \underline{\mathbf{A}}_v} &= (\mathbf{I}_{6 \times 16} \otimes \underline{\mathbf{A}}_v^{-1}) \underline{\mathbf{U}}_{16 \times 16} (\mathbf{I}_{6 \times 16} \otimes \underline{\mathbf{A}}_v^{-1}) (\mathbf{I}_{6 \times 16} \otimes \underline{\mathbf{Q}}_v) \end{aligned} \quad (18)$$

$$\frac{\partial \underline{\mathbf{P}}}{\partial \underline{\mathbf{Q}}} = \mathbf{T}_1 \left((-\underline{\mathbf{A}}_v^{-1})^T \right) \quad (19)$$

The first step in generalizing the method was to find the partial derivative of the general critical value shown in Eq. (10) in terms of $\underline{\mathbf{A}}_d$. First, the partial derivative of ψ in terms of $\underline{\mathbf{A}}_d$ is found using the matrix derivative product rule found in ¹² yielding

$$\frac{\partial \psi(\underline{\mathbf{A}}_d)}{\partial \underline{\mathbf{A}}_d} = \underline{\mathbf{U}}_{16 \times 16} (\mathbf{I}_{4 \times 4} \otimes \underline{\mathbf{x}}) \quad (20)$$

using again the matrix product rule, the partial derivative of η in terms of $\underline{\mathbf{P}}$ is found to be

$$\frac{\partial \eta(\underline{\mathbf{P}})}{\partial \underline{\mathbf{P}}} = (\mathbf{I}_{4 \times 4} \otimes \underline{\mathbf{e}}^T) \underline{\mathbf{U}}_{16 \times 16} \left(\mathbf{I}_{4 \times 4} \otimes \frac{\mathbf{I}_{4 \times 4}}{|\underline{\mathbf{e}}^T \underline{\mathbf{P}} \underline{\mathbf{B}}|} \right) - (\mathbf{I}_{4 \times 4} \otimes \underline{\mathbf{e}}^T \underline{\mathbf{P}}) \left[\frac{(\underline{\mathbf{e}}^T \underline{\mathbf{P}} \underline{\mathbf{B}})(\underline{\mathbf{e}}^T \underline{\mathbf{B}})}{|\underline{\mathbf{e}}^T \underline{\mathbf{P}} \underline{\mathbf{B}}|^3} \right] \quad (21)$$

Subsequently, using the matrix chain rule defined in ¹², the partial derivative of η in terms of $\underline{\mathbf{A}}_d$ is found to be

$$\frac{\partial \eta(\underline{\mathbf{P}})}{\partial \underline{\mathbf{A}}_d} = \mathbf{T}_3^{-1} \left(\frac{\partial \underline{\mathbf{P}}}{\partial \underline{\mathbf{A}}_d} \right) \left[\mathbf{I}_{4 \times 4} \otimes \mathbf{T}_1^{-1} \left(\frac{\partial \eta(\underline{\mathbf{P}})}{\partial \underline{\mathbf{P}}} \right) \right] \quad (22)$$

Finally, using the matrix product rule and Eqs. (19), (20), (21), and (22), the general partial derivative of the critical value in terms of $\underline{\mathbf{A}}_d$ is found to be

$$\begin{aligned} \frac{\partial a_{Dcrit}}{\partial \underline{\mathbf{A}}_d} = & \mathbf{T}_3^{-1} \left(\frac{\partial \underline{\mathbf{P}}}{\partial \underline{\mathbf{A}}_d} \right) \left[\mathbf{I}_{4 \times 4} \otimes \mathbf{T}_1^{-1} \left(\frac{\partial \eta(\underline{\mathbf{P}})}{\partial \underline{\mathbf{P}}} \right) \right] \left[\mathbf{I}_{4 \times 4} \otimes (\underline{\mathbf{A}}_d \mathbf{x} - \mathbf{f}(\mathbf{x}) + \underline{\mathbf{B}} \mathbf{u}_d) \right] + \\ & \left[\mathbf{I}_{4 \times 4} \otimes \frac{\mathbf{e}^T \underline{\mathbf{P}}}{\mathbf{e}^T \underline{\mathbf{P}} \underline{\mathbf{B}}} \right] \underline{\mathbf{U}}_{16 \times 16} (\mathbf{I}_{4 \times 4} \otimes \mathbf{x}) \end{aligned} \quad (23)$$

The second step for generalizing the methods is to find the partial derivative of the general critical value shown in Eq. (10) in terms of $\underline{\mathbf{Q}}$. First, using Eqs. (19), (21), and the matrix chain rule, the partial derivative of η in terms of $\underline{\mathbf{Q}}$ is found

$$\frac{\partial \eta(\underline{\mathbf{P}})}{\partial \underline{\mathbf{Q}}} = \mathbf{T}_3^{-1} \left(\mathbf{T}_1 \left((-\underline{\mathbf{A}}_v^{-1})^T \right) \right) \left[\mathbf{I}_{4 \times 4} \otimes \mathbf{T}_1^{-1} \left(\frac{\partial \eta(\underline{\mathbf{P}})}{\partial \underline{\mathbf{P}}} \right) \right] \quad (24)$$

The partial derivative of ψ in terms of $\underline{\mathbf{Q}}$ is a zero matrix since ψ is not a function of $\underline{\mathbf{Q}}$. Finally, using Eq. (24) and the matrix chain rule, the general partial derivative of the critical value in terms of $\underline{\mathbf{Q}}$ is found to be

$$\frac{\partial a_{Dcrit}}{\partial \underline{\mathbf{Q}}} = \mathbf{T}_3^{-1} \left(\mathbf{T}_1 \left((-\underline{\mathbf{A}}_v^{-1})^T \right) \right) \left[\mathbf{I}_{4 \times 4} \otimes \mathbf{T}_1^{-1} \left(\frac{\partial \eta(\underline{\mathbf{P}})}{\partial \underline{\mathbf{P}}} \right) \right] \left[\mathbf{I}_{4 \times 4} \otimes (\underline{\mathbf{A}}_d \mathbf{x} - \mathbf{f}(\mathbf{x}) + \underline{\mathbf{B}} \mathbf{u}_d) \right] \quad (25)$$

Adaptive Lyapunov Control Strategy

The same adaptation designed and presented by the authors in ^{1,2} is used here. By calculating the general partial derivatives defined in Equations (23) and (25), the entries of the matrices $\underline{\mathbf{Q}}$ and $\underline{\mathbf{A}}_d$, to which a_{Dcrit} is the most sensitive are identified (those entries which have the largest partial derivative). Once these entries are identified, the one with the highest partial derivative is selected, and slightly modified by a small value ($\delta_A = 10^{-6}$ for $\underline{\mathbf{A}}_d$ and $\delta_Q = 10^{-6}$ for $\underline{\mathbf{Q}}$). The sign of this modification is chosen such that it reduces the derivative of a_{Dcrit} , thus inducing a downward trend in the behavior of the critical value for the magnitude of the differential acceleration. By reducing this critical value, the overall robustness of the controller is improved since the control margin, that is the difference between the actual value of the differential drag acceleration and the critical value, is increased. The adaptive variations in the $\underline{\mathbf{Q}}$ and $\underline{\mathbf{A}}_d$ are expressed as:

$$\frac{dA_{ij}}{dt} = \kappa_A \left[-\text{sign} \left(\frac{\partial a_{Dcrit}}{\partial A_{ij}} \right) \delta_A \right], \quad \frac{dQ_{ij}}{dt} = \kappa_Q \left[-\text{sign} \left(\frac{\partial a_{Dcrit}}{\partial Q_{ij}} \right) \delta_Q \right] \quad (26)$$

where κ_A and κ_Q are defined by

$$\kappa_A = \begin{cases} 1 & \text{if } \left| \frac{\partial a_{Dcrit}}{\partial A_{ij}} \right| > \left| \frac{\partial a_{Dcrit}}{\partial A_{kl}} \right| \text{ for } i, j \neq k, l, \\ 0 & \text{else} \end{cases}, \quad (27)$$

$$\kappa_Q = \begin{cases} 1 & \text{if } \left| \frac{\partial a_{Dcrit}}{\partial Q_{ij}} \right| > \left| \frac{\partial a_{Dcrit}}{\partial Q_{kl}} \right| \text{ for } i, j \neq k, l, \\ 0 & \text{else} \end{cases}$$

The adaptation is implemented such that the modified \underline{Q} and \underline{A}_d matrices still satisfy their requirements of positive definiteness and symmetry for \underline{Q} and for \underline{A}_d being Hurwitz. Evidently, the adaptations of the \underline{Q} and \underline{A}_d matrices also affect the surface activation strategy since they cause variations in \underline{P} which is used for the surface activation strategy (see Eq. (9)). In other words, the adaptations of the matrices \underline{Q} and \underline{A}_d result in an adaptation of the quadratic Lyapunov function shown in Eq. (7). The adaptations are applied at the same time that the drag surface activation strategy is applied, that is every 10 minutes.

V. NUMERICAL SIMULATIONS RESULTS

For all the simulations, the guidance and control algorithms have been programmed in MATLAB. These algorithms interact with STK via STK Connect. STK's High-Precision Orbit Propagator (HPOP) has been used for modeling the mechanics of the maneuver, including J_2 perturbations, solar pressure radiation and variable atmospheric drag using the empirical NRLMSISE-00 model. For all of the simulations the adaptive Lyapunov controller using the generalized partial derivatives was compared to the Lyapunov controller presented in ².

Both adaptive and non-adaptive Lyapunov controllers can be implemented in the following configurations:

- 1) The controller is used to force the nonlinear system to directly track the analytically generated guidance trajectory
- 2) The controller forces the nonlinear system to track the trajectory of the reference model which is tracking the analytically generated guidance trajectory.
- 3) The controller forces the nonlinear system to go to a desired final state (regulation)

The initial orbital elements of the target (center of the LVLH frame) and other parameters for the numerical simulations are shown in Table 1. The target and chaser spacecraft are assumed to be identical, therefore drag coefficient and frontal areas for all surface configurations are the same. The initial relative position and velocity of the chaser in the LVLH frame are shown in Table 2 (the same initial state was used in previous work in ¹, ² and ⁸). For all simulations the initial \underline{Q} matrix was the identity matrix times 10^2 .

Table 1. Spacecraft Parameters

Parameter	Value
Second zonal harmonic J_2	1.08E-03(from ¹³)
Radius of the Earth R (km)	6378.1363
Gravitational parameter μ (km ³ /sec ²)	398600.4418
Target's inclination (deg)	98
Target's semi-major axis (km)	6778
Target's right ascension of the ascending node (deg)	262
Target's argument of perigee (deg)	30
Target's true anomaly (deg)	25
Target's eccentricity	0
v_s (km/sec)	7.68
m (kg)	10
S_{\min} surface retracted (m ²)	0.5
S_{\max} surface deployed (m ²)	2.5
$C_{D\min}$	1.5
C_{D0}	2
$C_{D\max}$	2.5

Table 2. Initial conditions in the LVLH frame

Parameter	Rendezvous	Fly-Around	Re-Phase
x (km)	-1	0	0
y (km)	-2	-4.25	-1.9
\dot{x} (km/sec)	4.8E-007	0	0
\dot{y} (km/sec)	1.70E-04	0	0

Re-Phase Maneuver

In this maneuver, both target and chaser spacecraft start at the same orbit but with a difference in their polar angles (true anomaly) at a given time, the maneuver consists in changing the value of this difference. In the LVLH plane the spacecraft start with zero relative position in the x direction (radial) but with a difference in the y direction (along track), thus the objective of the maneuver is to change this difference in the y direction while maintaining zero relative position in the x direction. For the simulation in STK, the initial difference in the y was -1.9km and the desired final difference was 3km (Figure 2). Both the Lyapunov and adaptive Lyapunov controller have been used in simulations for the re-phase maneuver (Figure 3, Figure 4). The controllers are used to regulate (third configuration) the error between the simulated relative positions and velocities and the desired final relative positions and velocities. For this maneuver the R_{LQR} value used to obtain the initial \underline{A}_d was 10^{18} .

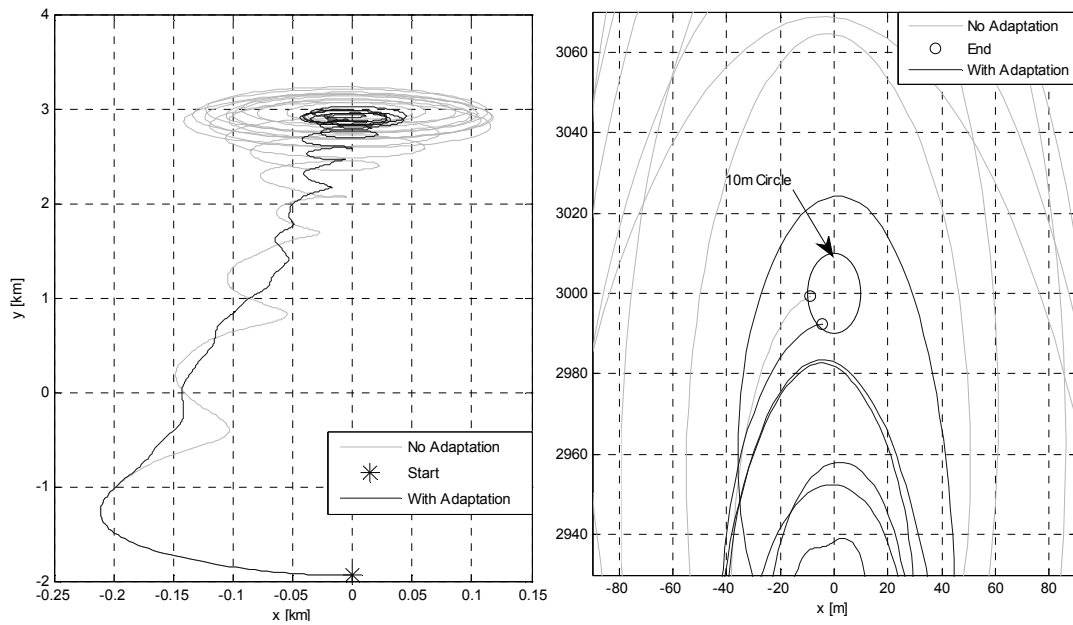


Figure 2. Re-Phase trajectory in the x-y plane: (left) complete maneuver and (right) final stages of the maneuver

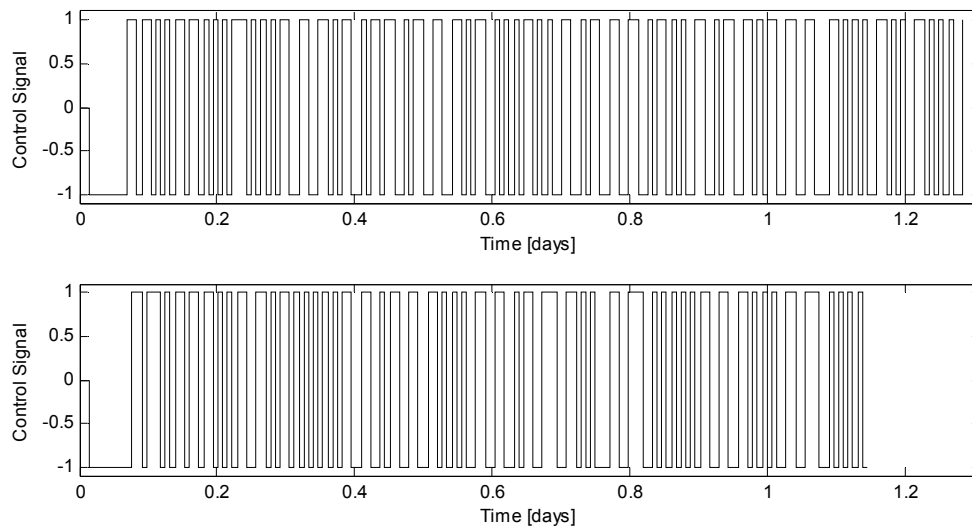


Figure 3. Re-Phase control signals: (top) non-adaptive Lyapunov controller and (bottom) adaptive Lyapunov controller

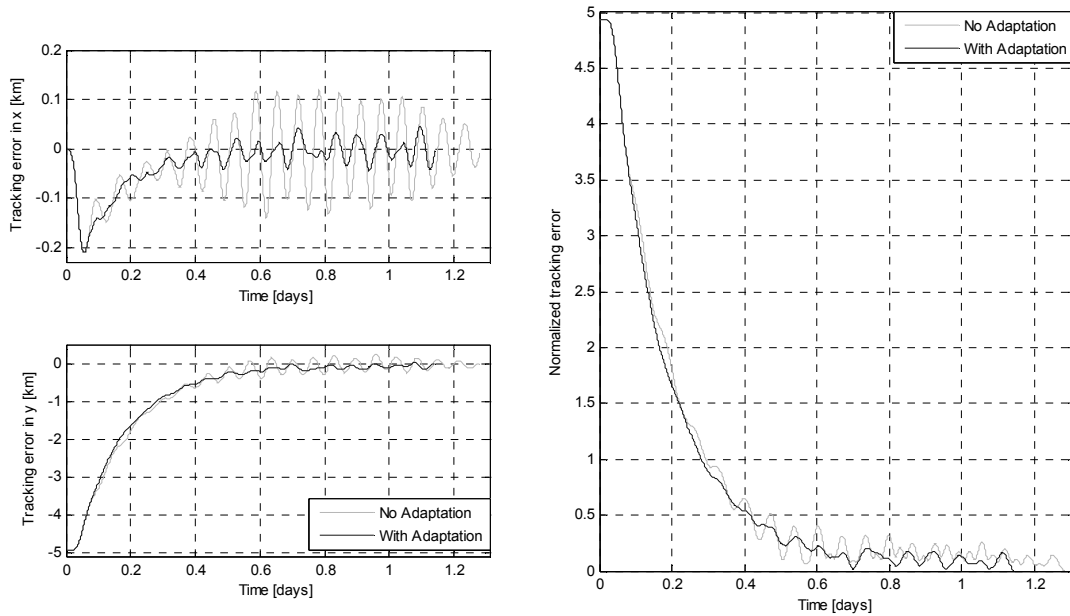


Figure 4. Re-Phase error over the entire maneuver: (left top) x error, (left bottom) y error, and (right) normalized error.

Fly-Around Maneuver

In this maneuver both spacecraft start at the same orbit but with a difference in their polar angles (true anomaly) at a given time. The objective of the maneuver is to follow a desired path in the LVLH plane which leads to a stable relative orbit of the chaser spacecraft around the target spacecraft (Figure 5). The guidance methodology developed by one of the authors in ¹⁴ has been selected for the fly-around maneuver. Both the Lyapunov and adaptive Lyapunov controller (with the generalized partial derivatives) have been used in simulations for the fly-around maneuver (Figure 6 and Figure 7). For this maneuver, regulation is no longer used since the desired final state is not a constant final relative position and velocity, but a stable relative orbit of the chaser around the target. Hence, the controllers force the nonlinear dynamics to follow the desired fly-around guidance and not just converge to a final state (first configuration). Moreover, the simulations are stopped 2.5 orbital periods after the guidance reaches the final stable orbit. For this maneuver the R_{LQR} value was 10^{18} .

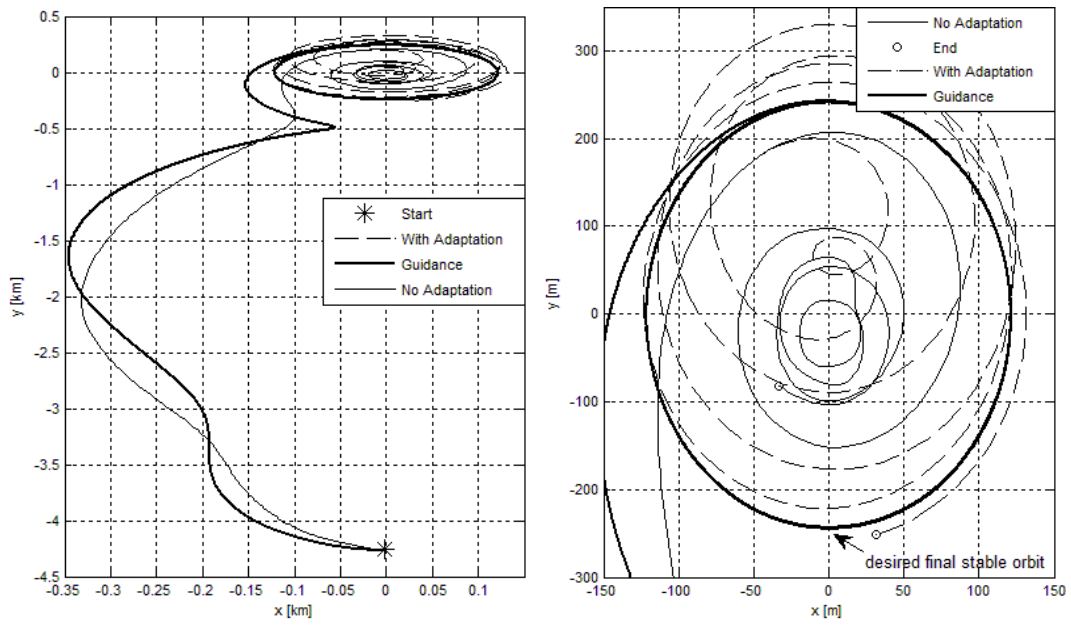


Figure 5. Fly-Around trajectory in the x–y plane: (left) complete maneuver and (right) final stages of the maneuver

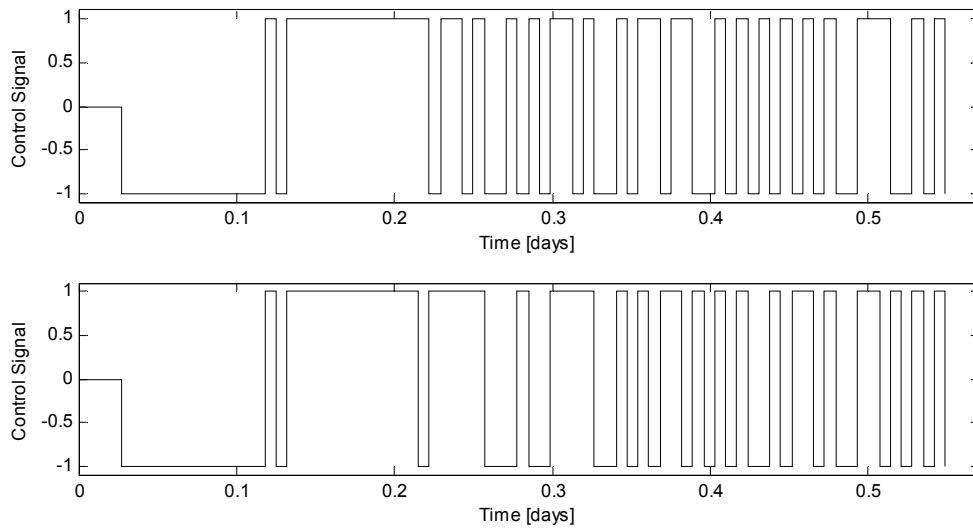


Figure 6. Fly-Around control signals: (top) non-adaptive Lyapunov controller and (bottom) adaptive Lyapunov controller

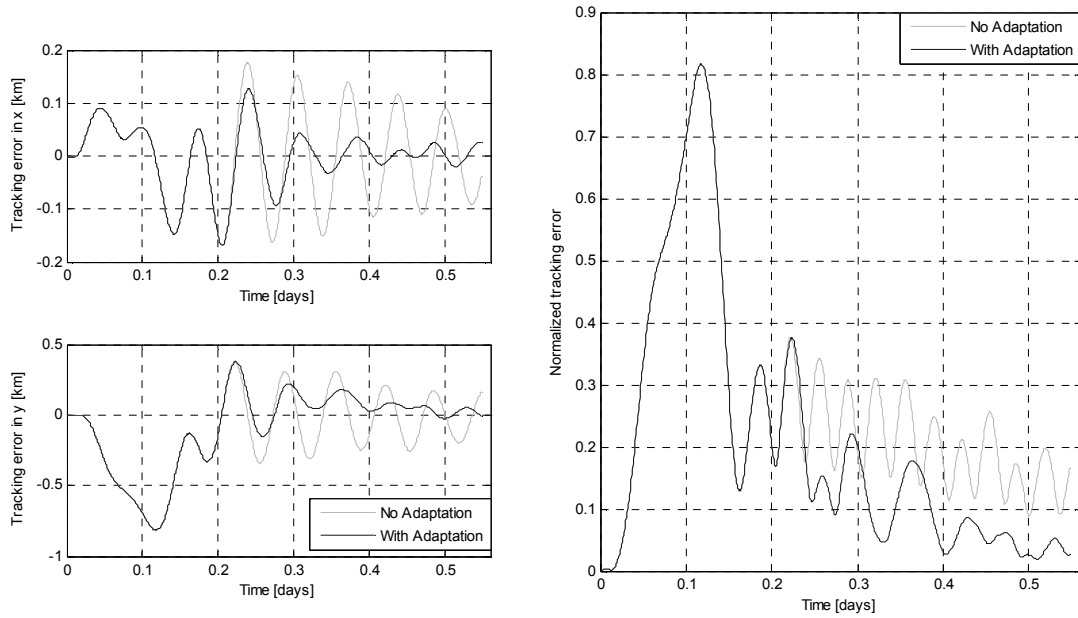


Figure 7. Fly-Around error over the entire maneuver: (left top) x error, and (left bottom) y error, (right) normalized error.

Rendezvous Maneuver

In this maneuver the spacecraft have a difference in both x and y directions. The objective of the maneuver is to drive both relative position and velocity to zero. This maneuver is particularly difficult to perform using differential drag since it requires reducing an initial difference in the x direction as well as in the y direction, and, as it was shown by the authors in ¹, ² and ⁸, this requires introducing large errors in the y direction. A guidance methodology (presented by one of the authors in ¹⁴) for rendezvous maneuvers using differential drag has been selected. In this simulation the controller forces the nonlinear system to track the trajectory of the reference model which is tracking the analytically generated guidance trajectory (second configuration). This configuration is quite useful since the behavior of the linear reference model when tracking the guidance is available a priori and, provided that the model is reasonable (i.e., not too demanding to track), it gives an insight into what the nonlinear system is expected to do. In order to illustrate the importance of the nature of the linear stable reference model, two cases for this maneuver were simulated. In Case 1 the R_{LQR} value used to obtain the initial \underline{A}_d was selected to give a less realistic (too demanding) linear reference model for the rendezvous ($R_{LQR}=1.6*10^{18}$), while in Case 2 this value was selected to obtain a better (more achievable) linear reference model ($R_{LQR}=1.5*10^{17}$).

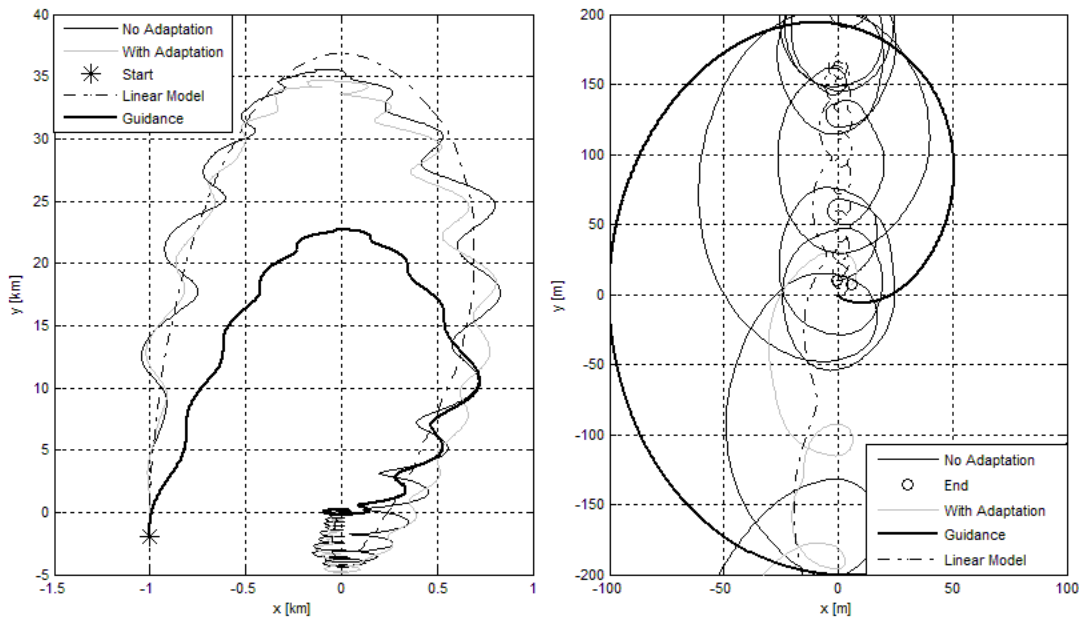


Figure 8. Rendezvous trajectory Case 1 in the x - y plane: (left) complete maneuver, and (right) final stages of the maneuver

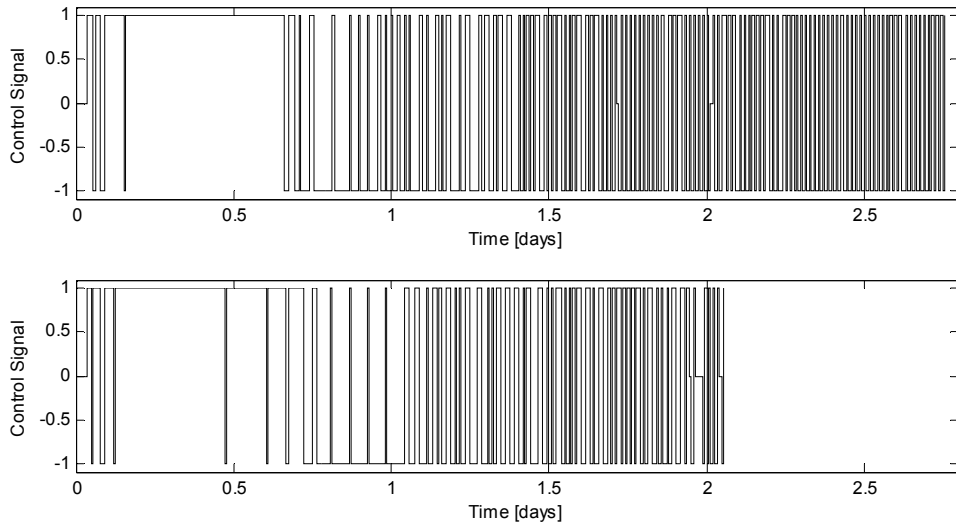


Figure 9. Rendezvous Case 1 control signals: (top) non-adaptive Lyapunov controller and (bottom) adaptive Lyapunov controller

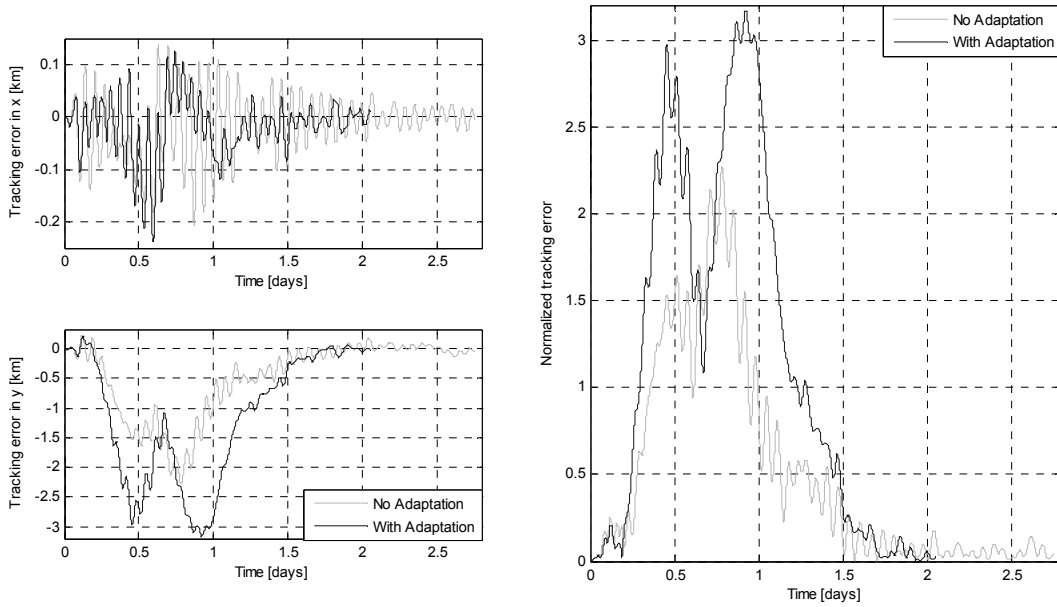


Figure 10. Rendezvous Case 1 error over the entire maneuver: (left top) x error, (left bottom) y error, and (right) normalized error.

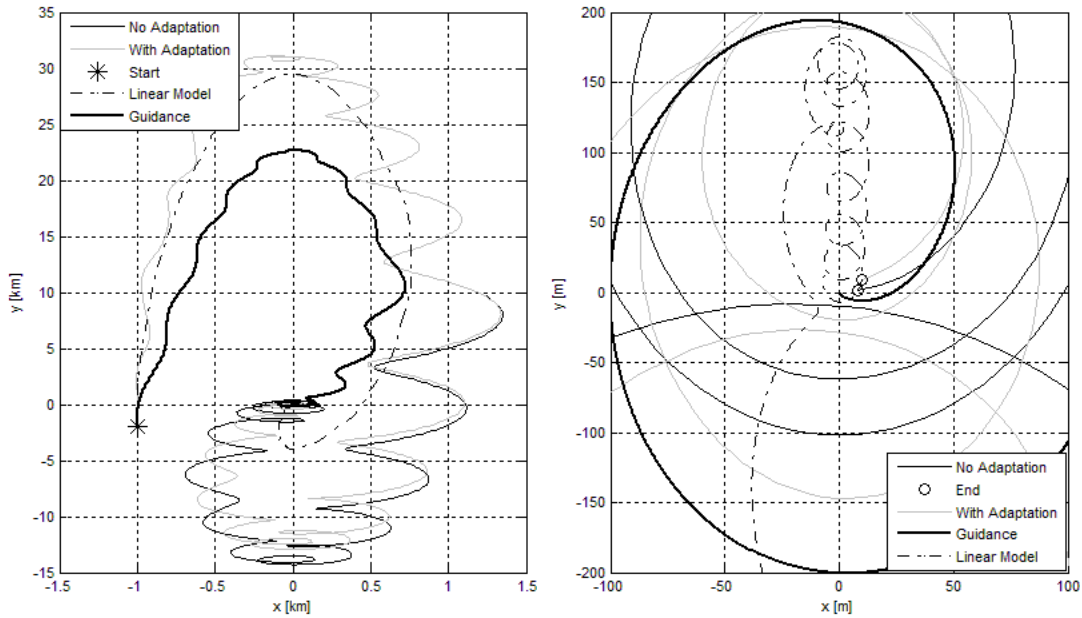


Figure 11. Rendezvous trajectory Case 2 in the x-y plane: (left) complete maneuver and (right) final stages of the maneuver

The tracking errors plots (Figure 4, Figure 7, Figure 10 and Figure 13) show that the adaptive controller allows for more accurate tracking of the trajectories, i.e. smoother controlled trajectories and shorter maneuvers. This behavior is also apparent in the plots from the fly-around maneuver since they show that the adaptive controller is able to get much closer to the desired final stable orbit than the non-adaptive one (Figure 5 right). The results also indicate that the selection of a reasonable initial linear reference model allows both Lyapunov controllers to force the non-linear dynamics to follow the reference model in a much more accurate way, that is following the

linear reference model more closely (see Figure 10 and Figure 13), in less time (see Figure 9 and Figure 12), and by introducing much less error in the y direction as the error in the x direction is being reduced (see Figure 10 and Figure 13). The parameters used to evaluate the performance of the controllers are the number of switches in the control (control effort), the duration of the maneuver, the means for the critical and actual value of the differential drag acceleration, and the difference between these two values (control margin). The actual value for the differential drag acceleration is available from the atmospheric model used; although, in practice this value would not be known a priori, and therefore it is not used by the controller.

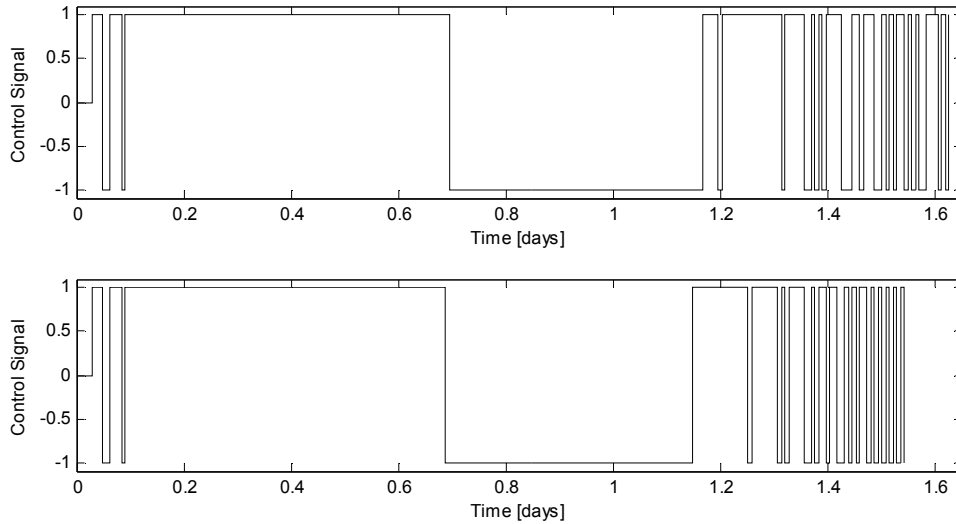


Figure 12. Rendezvous control Case 2 signals: (top) non-adaptive Lyapunov controller and (bottom) adaptive Lyapunov controller

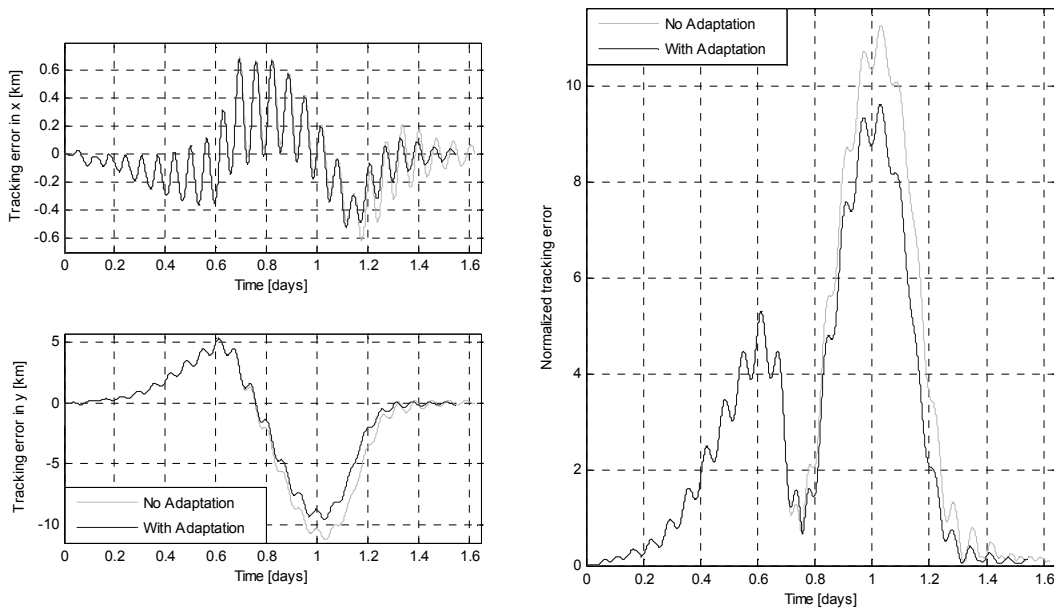


Figure 13. Rendezvous Case 2 error over the entire maneuver: (left top) x error, (left bottom) y error, and (right) normalized error.

Table 3. Performance parameters for all simulations

Parameter		Re-Phase (Regulation)	Fly-Around (Tracking Trajectory)	Rendezvous (Track- ing Dynamics)	
				Case 1	Case 2
Non-- Adaptive	Control Changes	124	41	239	37
	Time (hr)	30.7333	13.15	66.05	38.9167
	Drag Mean Critical value (m/s ²)	-2.93E- ⁰⁷	-6.50E- ⁰⁶	-1.16E- ⁰⁴	-1.71E- ⁰⁴
	Mean Actual Drag(m/s ²)	9.61E- ⁰⁶	3.38E- ⁰⁵	3.56E- ⁰⁵	3.50E- ⁰⁵
	Margin(m/s ²)	9.90E- ⁰⁶	4.03E- ⁰⁵	1.52E- ⁰⁴	2.06E- ⁰⁴
Adaptive	Control Changes	107	37	124	36
	Time (hr)	27.4	13.15	49.2833	37
	Drag Mean Critical value (m/s ²)	-6.54E- ⁰⁷	-7.23E- ⁰⁶	-1.50E- ⁰⁴	-1.74E- ⁰⁴
	Mean Actual Drag(m/s ²)	9.52E- ⁰⁶	3.38E- ⁰⁵	3.47E- ⁰⁵	3.50E- ⁰⁵
	Margin(m/s ²)	1.02E- ⁰⁵	4.10E- ⁰⁵	1.85E- ⁰⁴	2.09E- ⁰⁴

As it can be observed from the data in Table 3, the use of the adaptive controller reduced the control effort required to perform all three maneuvers with improvements of 13.7%, 9.8%, 48.2% and 2.7% for the re-phase, fly-around, Case 1 and Case 2 rendezvous maneuvers respectively. Moreover, the adaptive controller also reduced the duration of the maneuver with improvements of 10.9%, 25.4% and 4.9% for the re-phase, Case 1 and Case 2 rendezvous maneuvers respectively. There was no improvement in duration for the fly-around, since the simulation was not stopped when within 10m of the desired final position, but after 2.5 orbital periods after reaching the desired stable relative orbit. Additionally, the adaptive controller also was able to increase the control margin with an improvement of 2.7%, 1.8%, 18% and 1.6% for the re-phase, fly-around, Case 1 and Case 2 rendezvous maneuvers respectively. The fact that the improvements of the adaptive controller over the non-adaptive controller are much larger for Case 1 than Case 2 (rendezvous maneuver) is caused by the better selection of the initial linear reference model in Case 2. This leads to two observations: the first one is that the adaptation provides even better results as the accuracy of the linear reference degrades, and the second one is the substantial impact that the nature of the linear reference model (matrix \underline{A}_d) has on the performance of the Lyapunov controller. As was previously shown in ^{1, 2} (for a rendezvous maneuver using only regulation), the implementation of the adaptive controller yields improvements in terms of control effort, maneuver duration and control margin; however, the use of the general partial derivatives for the adaptation allows for performing more complicated maneuvers beyond those that can be achieved by using regulation.

VI. CONCLUSIONS

An adaptive Lyapunov controller based on differential drag is here generalized from the authors' previous work, to enable any planar spacecraft relative maneuvering. The development of analytical expressions for general partial derivatives of the differential drag critical value in terms of matrices \underline{Q} and \underline{A}_d (chosen by the control designer, i.e., independent variables), allows for the implementation of the adaptive Lyapunov controller, for tracking a trajectory, the dynamics of a reference model, or simply regulating to a desired final state. Consequently, the adaptive Lyapunov controller can be used for various propellant-less autonomous relative maneuvers within the orbital plane using differential drag as the source of control force. The results for the re-phase, fly-around, and the rendezvous maneuvers indicate that the implementation of the adaptive Lyapunov controller allows for smoother maneuvers with less duration, less actuation, and greater

control margin for the three different controller configurations studied. The use of the general derivatives will allow for the implementation of the adaptive Lyapunov controller in maneuvers, in which a specific path is desired, consequently, opening the possibilities for many other maneuvers using differential drag, provided that they are confined to the orbital plane. The results also confirm the importance of the linear reference model on the performance of both adaptive and non-adaptive controllers, representing an important topic for further investigation.

ACKNOWLEDGEMENTS

The authors wish to acknowledge the Air Force Office of Scientific Research for sponsoring this investigation under the Young Investigator Program (award no. FA9550-12-1-0072).

REFERENCES

1. Perez, D., Bevilacqua, R., "Differential Drag Spacecraft Rendezvous using an Adaptive Lyapunov Control Strategy", *Acta Astronautica* 83 (2013) 196–207 <http://dx.doi.org/10.1016/j.actaastro.2012.09.005>.
2. Perez, D., Bevilacqua, R., "Differential Drag Spacecraft Rendezvous using an Adaptive Lyapunov Control Strategy", paper IAA-AAS-DyCoSS1-09-05, 1st International Academy of Astronautics Conference on Dynamics and Control of Space Systems – DyCoSS'2012, Porto, Portugal, 19-21 March 2012. WINNER OF THE BEST STUDENT PAPER AWARD FOR THE CATEGORY: SPACECRAFT GUIDANCE, NAVIGATION, AND CONTROL.
3. Leonard, C. L., Hollister, W., M., and Bergmann, E. V. "Orbital Formationkeeping with Differential Drag". *AIAA Journal of Guidance, Control and Dynamics*, Vol. 12 (1) (1989), pp.108–113.
4. Maclay, and C. Tuttle, "Satellite Station-Keeping of the ORBCOMM Constellation Via Active Control of Atmospheric Drag: Operations, Constraints, and Performance," *Advances in the Astronautical Sciences*, Vol. 120, Part I, 2005.
5. De Ruiter, A., Lee, J., Ng, A., "A Fault-tolerant magnetic spin stabilizing controller for the JC2Sat-FF Mission". *AIAA guidance, navigation and control conference and exhibit*, Honolulu, Hawaii, 18–21 August 2008.
6. Kumar, B., Ng, A., Yoshihara, K., De Ruiter, A., "Differential Drag as a Means of Spacecraft Formation Control," *Proceedings of the 2007 IEEE Aerospace Conference*, Big Sky, MT, March 3-10, 2007.
7. Brill, J. (March 11, 2012). *About SSCO*. Available: <http://sso.gsfc.nasa.gov/about.html>. Last accessed March 11, 2012.
8. Perez, D., Bevilacqua, R., "Lyapunov-based Spacecraft Rendezvous Maneuvers using Differential Drag", AIAA-2011-6630 paper, *AIAA Guidance, Dynamics and Control Conference 2011*, Portland, OR.
9. Bevilacqua, R., Romano, M., "Rendezvous Maneuvers of Multiple Spacecraft by Differential Drag under J_2 Perturbation", *AIAA Journal of Guidance, Control and Dynamics*, vol.31 no.6 (1595-1607), 2008.
10. Schweighart, S. A., and Sedwick, R. J., "High-Fidelity Linearized J_2 Model for Satellite Formation Flight," *Journal of Guidance, Control, and Dynamics*, Vol. 25, No. 6, 2002, pp. 1073–1080.
11. Curti, F., Romano, M., Bevilacqua, R., "Lyapunov-Based Thrusters' Selection for Spacecraft Control: Analysis and Experimentation", *AIAA Journal of Guidance, Control and Dynamics*, Vol. 33, No. 4, July–August 2010, pp. 1143-1160.
12. Graham, Alexander. *Kronecker Products and Matrix Calculus: With Applications*. Chichester: Horwood, 1981. Print.
13. Vallado, D.A.: *Fundamentals of Astrodynamics and Applications*, 2nd ed. Microcosm Press, Hawthorne (2004).
14. Bevilacqua, R., "Spacecraft Planar Re-phasing Guidance and Control using Input Shaping and Differential Drag", in *final preparation for AIAA Journal of Guidance, Control, and Dynamics*.
15. Bevilacqua, R., Hall, J., S., Romano, M., "Multiple Spacecraft Assembly Maneuvers by Differential Drag and Low Thrust Engines", *Celestial Mechanics and Dynamical Astronomy (2010)* 106:69–88, DOI: 10.1007/s10569-009-9240-3.